International Tables for Crystallography (2012). Vol. F, Section 6.2.1, pp. 168–172.

Chapter 6.2. Neutron sources

B. P. Schoenborn and R. Knott

6.2.1. Reactors

The generation of neutrons by steady-state nuclear reactors is a well established technique (Bacon, 1962; Kostorz, 1979; Pynn, 1984; Carpenter & Yelon, 1986; Windsor, 1986; West, 1989). Reactor sources that play a major role in neutron-beam applications have a maximum unperturbed thermal neutron flux, $\varphi_{\rm th}$, within the range $1 < \varphi_{\rm th} < 20 \times 10^{14}$ cm^{-2} s^{-1}. A research reactor is essentially a matrix of fuel, coolant, moderator and reflector in a well defined geometry (Fig. 6.2.1.1). The fuel is uranium, and neutron-induced fission in the isotope ^{235}U produces a number of prompt and delayed neutrons (slightly more than a total of two) and, on average, one of these is required to maintain the steady-state chain reaction (*i.e.* criticality). The heat generated (∼200 MeV per fission event) must be removed, hence the need for an efficient coolant. In practice, the simultaneous requirements of complex thermal hydraulics and nuclear reaction kinetics must be addressed. The neutrons produced in the fission event have a mean energy of ∼1 MeV, and a material is required to reduce this energy to ∼25 MeV to take advantage of the larger fission cross section of ^{235}U in the 'thermal' energy range. Such a moderator is composed of a material rich in light nuclei, so that a large fraction of the neutron energy is transferred per collision.

There is an inherent maximum in neutron flux density imposed by the fission process (the number of excess neutrons produced per fission event), by the reduced density of neutron-generation material required for cooling purposes and by the heat-removal capacity of suitable coolants. Detailed design of reactor systems is essential to obtain the correct balance.

6.2.1.1. Basic reactor physics

Reactor physics is the theoretical and experimental study of the neutron distributions in the energy, spatial and time domains (Soodak, 1962; Jakeman, 1966; Akcasu *et al.*, 1971; Glasstone & Sesonske, 1994). The fundamental relation describing neutron kinetics is the Boltzmann transport equation (*e.g.* Spanier & Gelbard, 1969; Stamm'ler & Abbate, 1983; Weisman, 1983; Lewis & Miller, 1993). In theory, the transport equation describes the life of the neutron from its birth as a high-energy component of the fission process, through the various diffusion and moderation processes, until its ultimate end in (i) the chain reaction, (ii) leakage into beam tubes, or (iii) parasitic absorption (Williams, 1966). In practice, the complex nuclear reactions and the geometrical configurations of the component materials are such that a rigorous theoretical analysis is not always possible, and simplifying approximations are necessary. Nevertheless, well proven algorithms have been developed, and many have been included in computer codes (*e.g.* Hallsall, 1995).

On examination of the factors that influence the neutron flux distribution, there are three distinct but interdependent functions performed by the coolant, moderator and reflector. The coolant/moderator is of major importance in the fuelled region to sustain optimum conditions for the chain reaction, and the moderator/reflector is important in the regions surrounding the central core (Section 6.2.1.2). It should be noted that reactors for neutron-beam applications must be substantially undermoderated in order to provide a fast neutron flux at the edge of the core, which can be thermalized at the entry to the beam tubes. Most research reactors use H_2O or D_2O as the coolant/moderator.

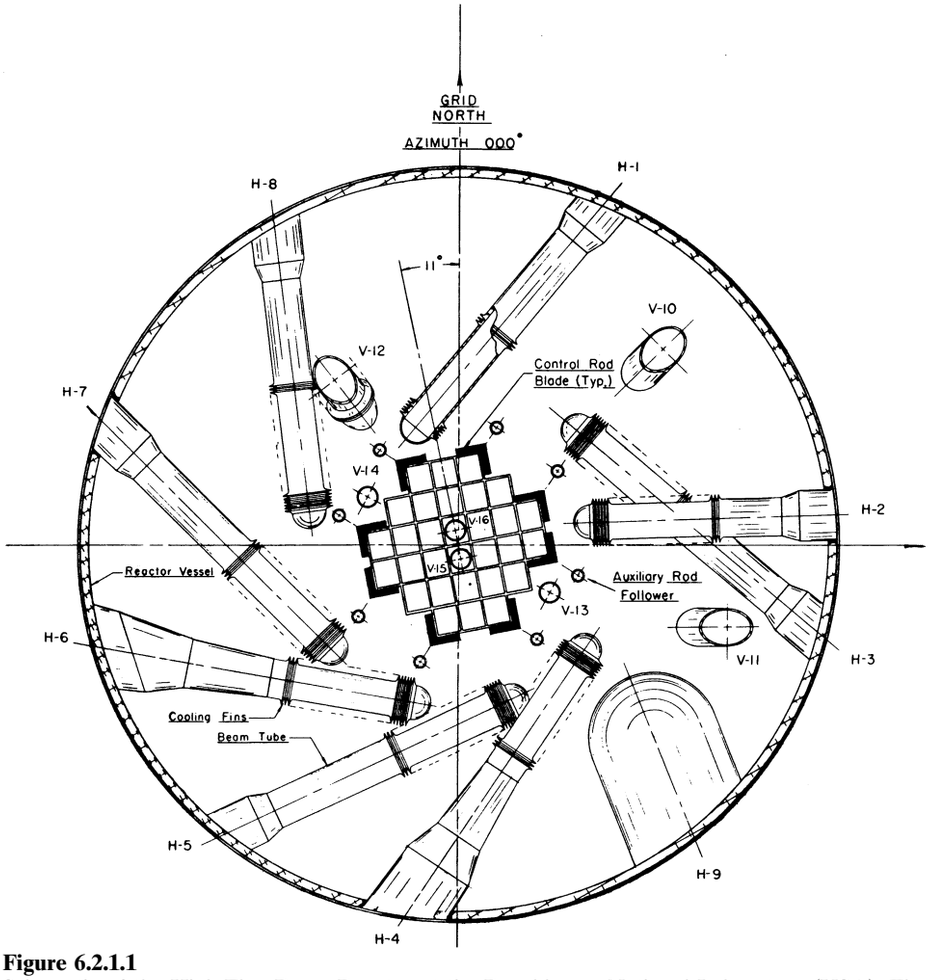

Figure 6.2.1.1
Schematic of the High Flux Beam Reactor at the Brookhaven National Laboratory (USA). The central core region (48 cm in diameter and 58 cm high) contains 28 fuel elements in an array surrounded by an extended D_2O moderator/reflector region. The diameter of the reactor vessel is approximately 2 m. All but one of the beam tubes are tangentially oriented with respect to the core. The cold neutron source is located in the H9 beam tube.

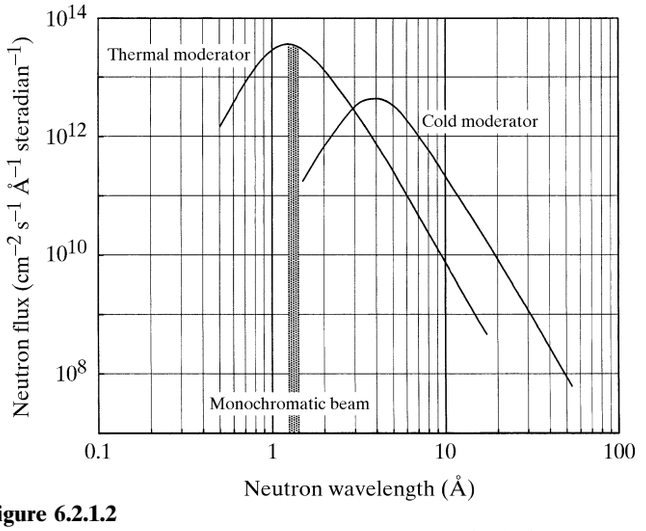

Figure 6.2.1.2
Neutron wavelength distributions for a thermal (310 K) and a cold (30 K) neutron moderator in a 'typical' dedicated beam reactor. The Maxwellian distribution merges with a $1/E$ slowing-down distribution at shorter wavelengths. A wavelength distribution for a monochromatic beam application on a thermal source is illustrated. It should be noted that, depending on the value of the mean wavelength for the monochromatic beam, harmonic contamination may be significant.

6.2.1.2. Moderators for neutron scattering

The moderator/reflector serves to modify the energy distribution of fast neutrons leaking from the central core, returning a significant number of thermalized neutrons to the core region to provide for criticality with a smaller inventory of fuel and providing excess neutrons for a range of applications, including neutron-beam applications. The moderator/reflector may be H_2O, D_2O, Be, graphite or a combination of these. Almost all choices have been used; however, the optimum is not achieved with any choice, and priorities must be set in terms of neutron-beam performance, other source activities and the reactor fuel cycle.

For neutron-beam applications, H_2O is the preferred reflector material since the moderation length is large and the absorption cross section low. Consequently, the thermal neutron flux peak is rather broad and occurs relatively distant from the core. While the exact position of the peak depends on the reactor core design, the peak width has a major impact on beam-tube orientation (Section 6.2.1.3). The combination of D_2O coolant/moderator–D_2O moderator/reflector provides a distinct advantage; however, for a number of technical reasons, the H_2O–D_2O combination is becoming more common, with the D_2O in a closed vessel surrounding the central H_2O-cooled core.

6.2.1.2.1. Thermal moderators

Neutrons thermalized within a 'semi-infinite' moderator/reflector typical of a steady-state reactor source establish an equilibrium Maxwellian energy distribution characterized by the temperature (T) of the moderator (Fig. 6.2.1.2). The wavelength, λ_m, at which the above distribution has a maximum is given by

$$\lambda_m = h/(5k_B T m_n)^{1/2}.$$

Depending on the width of the moderator and its composition, the Maxwellian distribution merges with the $1/E$ slowing-down distribution from the reactor core to give a total distribution at the beam-tube entry.

Clearly, the neutron wavelength distribution will depend on the local equilibrium conditions. Since steady-state reactors typically operate with moderator/reflector temperatures in the range 308–323 K, the corresponding λ_m is about 1.4 Å (Fig. 6.2.1.2). However, it is possible to alter the neutron distribution by re-thermalizing the neutrons in special moderator regions, which are either cooled significantly below or heated significantly above the average moderator temperature. One such device of prime importance is the cold moderator in the form of a cold source.

6.2.1.2.2. Cold moderators

The thermal neutron distribution shown in Fig. 6.2.1.2 is not ideal for all experiments, since the flux of 5 Å neutrons is almost two orders of magnitude less than the peak. The solution is to introduce a cold region in the moderator/reflector. This is typically a volume of liquid H_2 or D_2 at ~10–30 K, and a Maxwellian distribution around this temperature results in a λ_m of ~4 Å. The geometric design of a cold-source vessel has been shown to be very important, with substantial gains in neutron flux obtained by innovative design. A re-entrant geometry approximately 20 cm in diameter filled with liquid D_2 at 10 K provides optimum neutron thermalization with superior coupling to neutron guides (Section 6.2.1.3.5) (Ageron, 1989; Lillie & Alsmiller, 1990; Alsmiller & Lillie, 1992).

6.2.1.3. Beamline components

Until recently, instrument design has been largely based on experience; however, in many cases, it is now possible to formulate a comprehensive description of the instrument and explore the impact of various parameters on instrument performance using an extensive array of computational methods (Johnson & Stephanou, 1978; Sivia *et al.*, 1990; Hjelm, 1996). In practice, it is the instrument design that provides access to the fundamental scattering processes, as briefly outlined in the following.

If a neutron specified by a wavevector $\mathbf{k}_1$ is incident on a sample with a scattering function $S(\mathbf{Q}, \omega)$, all neutron scattering can be reduced to the simple form

$$\frac{\mathrm{d}^2\sigma}{\mathrm{d}\Omega\ \mathrm{d}E} = AS(\mathbf{Q}, \omega),$$

where A is a constant containing experimental information, including instrumental resolution effects. The basic quantity to be measured is the partial differential cross section, which gives the fraction of neutrons of incident energy E scattered into an element of solid angle Ω with an energy between E' and $E' + \mathrm{d}E'$. The momentum transfer, $\mathbf{Q}$, is given in Fig. 6.2.1.3(*a*). The primary aim of a neutron-scattering experiment is to measure $\mathbf{k}_2$ to a predetermined precision (Bacon, 1962; Sears, 1989) (Fig. 6.2.1.3*b*). A generic neutron-scattering instrument used to achieve this aim is illustrated in Fig. 6.2.1.4. The instrument resolution function will be determined by uncertainties in $\mathbf{k}_1$ and $\mathbf{k}_2$, which are a direct consequence of (i) measures to increase the neutron flux at the sample position (to maximize wavelength spread, beam divergence, monochromator mosaic, for example) and (ii) uncertainties in geometric parameters (flight-path lengths, detector volume *etc.*).

6.2.1.3.1. Collimators and filters

In general, neutron-beam applications are flux-limited, and a major advantage will be realized by adopting advanced techni-

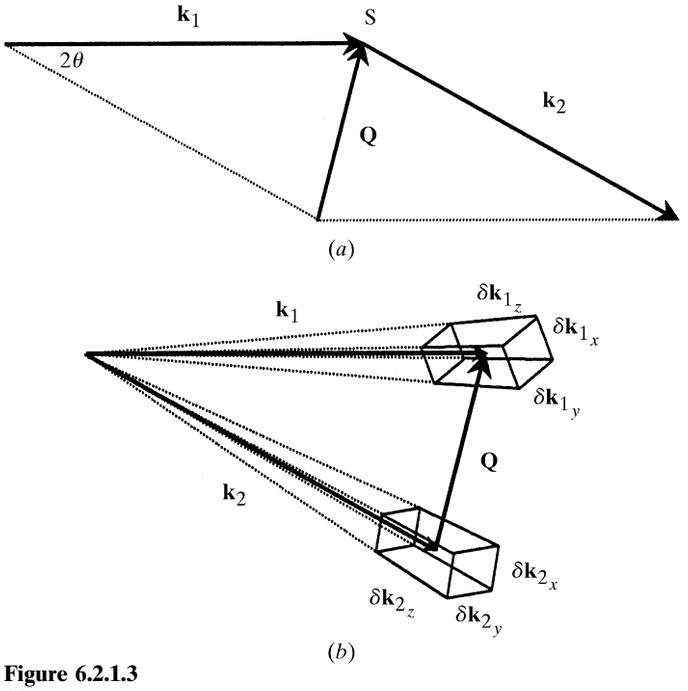

Figure 6.2.1.3
(*a*) Schematic vector diagram for an elastic neutron-scattering event. A neutron, $\mathbf{k}_1$, is incident on a sample, S, and a scattered neutron, $\mathbf{k}_2$, is observed at an angle 2θ leading to a momentum transfer, $\mathbf{Q}$. (*b*) Schematic of an elastic neutron-scattering event illustrating the consequences of uncertainty in defining the incident neutron, $\mathbf{k}_1$, and determining the scattered neutron, $\mathbf{k}_2$. The volumes ($\delta\mathbf{k}_{1_x}$, $\delta\mathbf{k}_{1_y}$, $\delta\mathbf{k}_{1_z}$) and ($\delta\mathbf{k}_{2_x}$, $\delta\mathbf{k}_{2_y}$, $\delta\mathbf{k}_{2_z}$) constitute the instrument resolution function.

ques in flux utilization. A reactor neutron source is large, and stochastic processes dominate the generation, moderation and general transport mechanisms. Because of radiation shielding, background reduction and space requirements for scattering instruments, reactor beam tubes have a minimum length of 3–4 m and cannot exceed a diameter of about 30 cm. The useful flux at the beam-tube exit is thus between 10^{-5} and 10^{-6} times the isotropic flux at its entry.

The most important aspect of beam-tube design, other than the size, is the position and orientation of the tube with respect to the reactor core. The widespread utilization of D_2O reflectors enables significant gains to be obtained from tangential tubes with maximal thermal neutron flux, and minimal fast neutron and γ fluxes. A similar result is accomplished in a split-core design by orienting the beam tubes toward the unfuelled region of the reactor core (Prask *et al.*, 1993).

There are two major groups of neutron-scattering instruments: those located close to and those located some distance from the neutron source. The first group is located to minimize the impact of the inverse square law on the neutron flux, and the second group is located to reduce background and provide more instrument space. In both cases, the first beamline component is a collimator to extract a neutron beam of divergence α from the reactor environment. The collimator is usually a beam tube of suitable dimensions for fully illuminating the wavelength-selection device. The angular acceptance of a collimator is determined strictly by the line-of-sight geometry between the source and the monochromator. Some geometric focusing may be appropriate, and a Soller collimator may be used to reduce α without reducing the beam dimensions. For technical reasons, the primary collimator is essentially fixed in dimensions and secondary collimators of adjustable dimensions may be required in more accessible regions outside the reactor shielding.

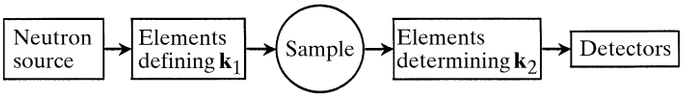

Figure 6.2.1.4
A generic neutron-scattering instrument illustrating the classes of facilities and operators important to instrument design and assessment. Each class should be optimized and integrated into the overall instrument description.

Neutron-beam filters are required for two main reasons: (i) to reduce beam contamination by fast neutron and γ radiation and (ii) to reduce higher- or lower-order harmonics from a monochromatic beam. Numerous single-crystal, polycrystalline and multilayer materials with suitable characteristics for filter applications are available (*e.g.* Freund & Dolling, 1995).

6.2.1.3.2. Crystal monochromators

The equilibrium neutron-wavelength distribution (Fig. 6.2.1.2) is a broad continuous distribution, and in most experiments it is necessary to select a narrow band in order to define $\mathbf{k}_1$. Neutron-wavelength selection can be achieved by Bragg scattering using single crystals to give well defined wavelengths; by polycrystalline material to remove a range of wavelengths; by a mechanical velocity selector; or by time-of-flight methods. The method chosen will depend on experimental requirements for the wavelength, λ, and wavelength spread, $\Delta\lambda/\lambda$.

Neutrons incident on a perfect single crystal of given interplanar spacing d will be diffracted to give specific wavelengths at angle 2θ according to the Bragg relation. A neutron beam, α_1, incident on a single crystal of mosaicity β will provide

$$\Delta\lambda/\lambda = [(\cot\theta\cdot\theta)^2 + (\Delta d/d)^2]^{1/2},$$

where

$$(\Delta\theta)^2 = \frac{\alpha_1^2\alpha_2^2 + \beta^2(\alpha_1^2 + \alpha_2^2)}{\alpha_1^2 + \alpha_2^2 + 4\beta^2}$$

and α_2 is the divergence of the (unfocused) diffracted beam.

Crystals for neutron monochromators must not only have a suitable d, but also high reflectivity and adequate β. Under these conditions, neutron beams with a $\Delta\lambda/\lambda$ of a few per cent are obtained. Typical crystals are Ge, Si, Cu and pyrolytic graphite. In order to increase the neutron flux at the sample, a number of mechanisms have been developed. These include focusing monochromatic crystals, frequently using Si or Ge (Riste, 1970; Mikula *et al.*, 1990; Copley, 1991; Magerl & Wagner, 1994; Popovici & Yelon, 1995), as well as stacked composite wafer monochromators (Vogt *et al.*, 1994; Schefer *et al.*, 1996).

One limitation of the use of crystal monochromators is the absence of suitable materials with large d. Indeed, the longest useable λ diffracted from pyrolytic graphite or Si is ~5–6 Å.

6.2.1.3.3. Multilayer monochromators and supermirrors

Multilayers are especially useful for preparing a long-wavelength neutron beam from a cold source and for small-angle scattering experiments in which $\Delta\lambda/\lambda$ of about 0.1 is acceptable (Schneider & Schoenborn, 1984). Multilayer monochromators are essentially one-dimensional crystals composed of alternating layers of neutron-different materials (*e.g.* Ni and Ti) deposited on a substrate of low surface roughness. In order to produce multilayers of excellent performance, uniform layers are required with low interface roughness, low interdiffusion between layers

and high scattering contrast. Various modifications (*e.g.* carbonation, partial hydrogenation) to the pure Ni and Ti bilayers improve the performance significantly by fine tuning the layer uniformity and contrast (Mâaza *et al.*, 1993). The minimum practical *d*-spacing is ∼50 Å and a useful upper limit is ∼150 Å. Multilayer monochromators have high neutron reflectivity (>0.95 is achievable), and their angular acceptance and bandwidth can be selected to produce a neutron beam of desired characteristics (Saxena & Schoenborn, 1977, 1988; Ebisawa *et al.*, 1979; Sears, 1983; Schoenborn, 1992*a*).

The supermirror, a development of the multilayer monochromator concept, consists of a precise number of layers with graded *d*-spacing. Such a device enables the simultaneous satisfaction of the Bragg condition for a range of λ and, hence, the transmission of a broader bandwidth (Saxena & Schoenborn, 1988; Hayter & Mook, 1989; Böni, 1997).

Polarizing multilayers and supermirrors (Schärpf & Anderson, 1994) facilitate valuable experimental opportunities, such as nuclear spin contrast variation (Stuhrmann & Nierhaus, 1996) and polarized neutron reflectometry (Majkrzak, 1991; Krueger *et al.*, 1996). Supermirrors consisting of Co and Ti bilayers display high contrast for neutrons with a magnetic moment parallel to the saturation magnetization and very low contrast for the remainder. With suitable modification of the substrate to absorb the antiparallel neutrons, a polarizing supermirror will produce a polarized neutron beam (polarization >90%) by reflection.

6.2.1.3.4. Velocity selectors

The relatively low speed of longer-wavelength neutrons (∼600 m s^{-1} at 6 Å) enables wavelength selection by mechanical means (Lowde, 1960). In general, there are two classes of mechanical velocity selectors (Clark *et al.*, 1966). Rotating a group of short, parallel, curved collimators about an axis perpendicular to the beam direction will produce a pulsed neutron beam with λ and $\Delta\lambda/\lambda$ determined by the speed of rotation. This is a Fermi chopper. An alternate method is to translate short, parallel, curved collimators rapidly across the neutron beam, permitting only neutrons with the correct trajectory to be transmitted. This is achieved in the helical velocity selector, where the neutron wavelength is selected by the speed of rotation and $\Delta\lambda/\lambda$ can be modified by changing the angle between the neutron beam and the axis of rotation (Komura *et al.*, 1983). The neutron beam is essentially continuous, the resolution function is approximately triangular and the overall neutron transmission efficiency exceeds 75% in modern designs (Wagner *et al.*, 1992).

6.2.1.3.5. Neutron guides

In order for a collimator to be effective, its walls must absorb all incident neutrons. The angular acceptance is strictly determined by the line-of-sight geometry. Neutron guides can be used to improve this acceptance dramatically and to transport neutrons with a given angular distribution, almost without intensity loss, to regions distant from the source (Maier-Leibnitz & Springer, 1963). The basic principle of a guide is total internal reflection. This occurs for scattering angles less than the critical angle, θ_c, given by

$$\theta_c = 2(1 - n)^{1/2},$$

where n is the (neutron) index of refraction related to the coherent scattering length, b, of the wall material, *viz*,

$$n = 1 - (\lambda^2 \rho b/2\pi),$$

where ρ is the atom number density (in cm^{-3}). Among common materials, Ni with $b = 1.03 \times 10^{-12}$ cm, in combination with suitable physico-chemical properties, provides the best option, with a critical angle $\theta_c = 0.1\lambda$ (in Å). The dependence of θ_c on λ implies that guides are more effective for long-wavelength neutrons. With the introduction of supermirror guides with up to four times the θ_c of bulk Ni, both thermal and cold neutron beams are being transported and focused with high efficiency (Böni, 1997).

While a straight guide transports long wavelengths efficiently, it continues to transport all neutrons within the critical angle, including non-thermal neutrons emitted within the solid angle of the guide. This situation may be modified significantly by introducing a curvature to the guide. Since a curved neutron guide provides a form of spectral tailoring (cutoff or bandpass filters), simulation is a distinct advantage in exploring the impact of guide geometry on neutron-beam quality (van Well *et al.*, 1991; Copley & Mildner, 1992; Mildner & Hammouda, 1992).

6.2.1.4. Detectors

The detection of thermal neutrons is a nuclear event involving one of only a few nuclei with a sufficiently large absorption cross section (^{3}He, ^{10}B, ^{6}Li, Gd and ^{235}U). The secondary products (fragments, charged particles or photons) from the primary nuclear event are used to determine the location. Depending on the geometry of the instrument, either a spatially integrating or a position-sensitive detector is required (Convert & Forsyth, 1983; Crawford, 1992; Rausch *et al.*, 1992). The relatively weak neutron source is driving instrument design towards maximizing the number of neutrons collected per unit time, and, in many cases, this leads to the use of multiwire or position-sensitive detectors. The main performance characteristics for detector systems are position resolution, number of resolution elements, efficiency, parallax, maximum count rate, dynamic range, sensitivity to γ background and long-term stability.

6.2.1.4.1. Multiwire proportional counters

The principles of a multiwire proportional counter (MWPC) are well established (Sauli, 1977) and have wide application. For thermal neutron detection (Radeka *et al.*, 1996), the reaction of choice is

$$^3\mathrm{He} + \mathrm{n} \rightarrow {}^3\mathrm{H} + \mathrm{p} + 764\ \mathrm{keV}.$$

The 191 keV triton and the 573 keV proton are emitted in opposite directions and create a charge cloud whose dimensions are determined primarily by the pressure of a stopping gas. Depending on the work function of the gas mixture, approximately 3×10^4 electron–ion pairs are created. Low-noise gas amplification of this charge cloud occurs in an intense electric field created in the vicinity of the small diameter (20–30 μm) anode wires (Radeka, 1988). Typical gas gains of ∼10–50 lead to a total charge on the anode of ∼50–100 fC. The efficiency of the detector is determined by the pressure of ^{3}He, and the spatial resolution and count-rate capability are determined by the detector geometry and readout system. The event decoding is selected from the time difference (Borkowski & Kopp, 1975), charge division (Alberi *et al.*, 1975), centroid-finding filter (Radeka & Boie, 1980), or wire-by-wire techniques (Jacobé *et al.*, 1983; Knott *et al.*, 1997). Present MWPC technology offers opportunities and challenges to design a detector system that is totally integrated into the instrument design and optimizes data

collection rate and accuracy (Schoenborn *et al.*, 1985, 1986; Schoenborn, 1992*b*).

A concept related to the MWPC is the micro-strip gas chamber (MSGC). With the MSGC, the general principles of gas detection and amplification apply; however, the anode is deposited on a suitable substrate (Oed, 1988, 1995; Vellettaz *et al.*, 1997). The MSGC can potentially improve the performance of the MWPC in some applications, particularly with respect to spatial resolution and count-rate capability.

6.2.1.4.2. Image plates

The principles underlying the operation of an image plate (IP) are presented in detail in Chapter 7.2. Briefly, the important difference between an IP for X-ray and neutron detection is the presence of a converter (either Gd_2O_3 or ^6Li). The role of the converter is to capture an incoming neutron and create an event within the IP that mimics the detection of an X-ray photon. For example, neutron capture in Gd produces conversion electrons that exit the Gd_2O_3 grains, enter neighbouring photostimulated luminescence (PSL) material and create colour centres to form a latent image (Niimura *et al.*, 1994; Takahashi *et al.*, 1996). A neutron IP may have a virtually unlimited area and a shape limited only by the requirement to locate the detection event in a suitable coordinate system. With a neutron-detection efficiency of up to 80% at ~1–2 Å, a dynamic quantum efficiency of ~25–30% can be obtained. The dynamic range is intrinsically $1{:}10^5$. The spatial resolution is primarily limited by scattering processes of the readout laser beam, and measured line spread functions are typically 150–200 μm. The γ sensitivity is high and may restrict the application to instruments with low ambient γ background.

Neutron IPs are integrating devices well suited to data-acquisition techniques with long accumulation times, such as Laue diffraction (Niimura *et al.*, 1997) and small-angle scattering. On-line readout is a distinct advantage (Cipriani *et al.*, 1997).

6.2.1.5. Instrument resolution functions

For accurate data collection, the instrument smearing contribution to the data must be known with some certainty, particularly when data are collected over an extended range with multiple instrument settings. A balance must be struck between instrument smearing and neutron flux at the sample position; however, careful instrument design can produce: (i) a good signal-to-background ratio, thereby partially offsetting the flux limitation, and (ii) facilities and procedures for determining the instrument resolution function (Johnson, 1986).

As an example, instrumental resolution effects in the small-angle neutron scattering (SANS) technique have been investigated in some detail. A 'typical' SANS instrument is located on a cold neutron source with an extended (and often variable) collimation system. The sample is as large as possible and the detector is large with low spatial resolution. The instrument is best described by pin-hole geometry. Three major contributions to the smearing of an ideal curve are: (i) the finite λ, (ii) $\Delta\lambda/\lambda$ of the beam and (iii) the finite resolution of the detector. Indirect Fourier transform, Monte Carlo and analytical methods have been developed to analyse experimental data and predict the performance of a given combination of resolution-dependent elements (*e.g.* Wignall *et al.*, 1988; Pedersen *et al.*, 1990; Harris *et al.*, 1995).

6.2.2. Spallation neutron sources

Another phenomenon, quite different from the fission process (Section 6.2.1), that will produce neutrons uses high-energy particles to interact with elements of medium to high mass numbers. This process, called spallation, was first demonstrated by Seaborg and Perlman, who showed that the bombardment of nuclei by high-energy particles results in the emission of various nucleons. The nuclear processes involved in spallation (Prael, 1994) are complex and are summarized in Fig. 6.2.2.1. These processes have been investigated in some detail, and excellent background information is available (Hughes, 1988; Carpenter, 1977; Windsor, 1981). Present-day spallation sources typically use high-energy protons from an accelerator to bombard a heavy-metal target, such as W or U, and come in two types, using either a pulsed proton beam (*e.g.* ISIS or LANSCE) or a 'continuous' proton beam (SINQ).

The high-energy neutrons produced by spallation are moderated in a reflector region to intermediate energies and then reduced to thermal energies in a hydrogenous medium called the moderator (Russell *et al.*, 1996). These thermal neutrons are then extracted *via* beam pipes. A typical layout of a target system with reflectors and moderators is shown in Fig. 6.2.2.2.

The neutrons produced by the proton pulse travel along beam pipes as a function of their velocity, proportional to their energy.

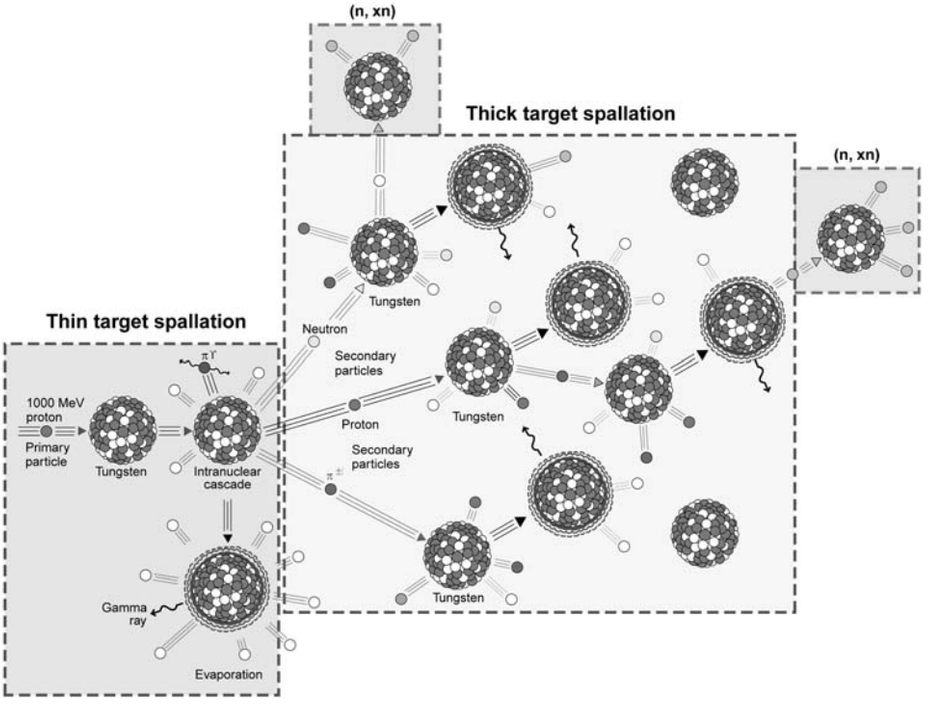

Figure 6.2.2.1
Schematic presentation of the various nuclear processes encountered in spallation. The numerical analysis of these processes is carried out by two Monte Carlo-based codes – the *LAHET* code models the higher-energy nuclear interactions, while the *HMCNP* code models the thermal interactions and the transport of neutrons to the sample.

references